COMPUTER-AIDED DESIGN & APPLICATIONS, 2016
VOL. 13, NO. 1, 86–94
http://dx.doi.org/10.1080/16864360.2015.1059199

Topology optimization for manufacturability based on the visibility map

Yonghua Chen, Jianan Lu and Ying Wei

The University of Hong Kong

ABSTRACT

As a popular and effective tool for structural design, topology optimization has been increasingly used for mechanical part design in recent years. However, the effectiveness of topology optimization in mechanical design has been seriously affected by the poor manufacturability of parts generated. In this study, manufacturability in the topology optimization process is described by using the concept of a visibility map. Apart from additive manufacturing, almost all manufacturing processes can be associated with a visibility map. A part generated by topology optimization must conform to the visibility map of a manufacturing process thus generating optimized design that is manufacturable by the proposed manufacturing process. Since the visibility map concept can be used to describe most manufacturing processes, the proposed approach can be used as a general method for all mechanical part design when topology optimization is needed.

KEYWORDS

topology optimization; manufacturability; visibility map

1. Introduction

The wide spread use of topology optimization in structural design has caught the attention of researchers in mechanical engineering design. Over the years, there are some reports about practical applications of topology optimization in aerospace [8], automotive [16] and prosthetics design [9], etc. However, current topology optimization methods have the tendency to generate hollow and framework-like features in the optimized design. To convert the optimized structure into a sensible mechanical design, manual intervention must be done. This process will defeat the purpose of optimization as the manually modified structure may not be the optimal any more.

To generate sensible mechanical parts directly from topology optimization, effort had been made to integrate manufacturing constraints into the structural optimization processes. Zuo et al had considered the minimum feature size and geometric symmetry as manufacturing constraints to generate parts that can be machined [21]. A hybrid of moving asymptotes and wavelets had been used to solve the topology optimization problem. Chang et al considered cost of manufacturing in their optimization process [2]. Niclas [10] and Zhou et al [20] had considered draw direction or draft angle as sample manufacturing constraints. Harzheim et al have reviewed optimization methods for cast parts [5]. Even more, some optimization software has been reported to incorporate manufacturing constraints for casting process [12]. All previous studies have considered only one or two constraints for a specific manufacturing process. No one has reported a general topology optimization approach that is applicable to most commonly used manufacturing processes.

In most manufacturing processes such as machining, casting/molding, or forging, etc, there are some primary directions. For instance, the tool approach directions for machining, parting directions for casting/molding, and punching direction for forging. Geometric features of a part design should be properly aligned with respect to these directions in order to be manufacturable. Inspired by this observation, this study proposes and implements a visibility map constrained topology optimization approach for mechanical part designs. The visibility map of a 3D object is generated on a unit sphere that encloses the object that is to be optimized [3,18]. Using visibility map, the complex problem of visibility can be addressed by simple spherical algorithms that invoke the intersection between the visibility map and a point, a great circle or s spherical rectangle.

2. Visibility

In practical manufacturing, different manufacturing processes may impose different constraints on part geometry and topology. The following will describe the visibility

CONTACT Yonghua Chen yhchen@hku.hk

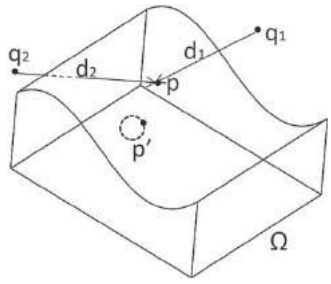

Figure 1. Diagram illustrating the visibility concept.

concept and how a manufacturing process is mapped onto a unit sphere.

2.1. Visibility

Given an object **Ω**, a point p on the boundary of **Ω** is visible to an exterior point q if no part of the line segment *pq* lies in the interior of **Ω** [3]. A point p is said to be completely invisible only if the segment *pq* intersects with the object **Ω**. The definition of visibility could be explained by Fig. 1. A point p on the curved surface of object **Ω** is visible by an exterior point q1 because no part of the line segment *pq1* lies in the interior of **Ω**. On the contrary, point p is invisible to point q2 since the line segment *pq2* intersects with **Ω**. For the point p' on the boundary of an internal void of **Ω**, all the line segments between p' and any exterior point will intersect with object **Ω**, therefore point p' is completely invisible.

In a practical manufacturing process, an object is said to be visible if no points on its surfaces is completely invisible to the process directions.

2.2. Visibility map

TC woo has developed the theory of visibility map (Vmap) [18]. For a point p on the surface **S** as in Fig. 2(a), let n be the normal and T be the tangent plane at the point p on the surface **S**. The point p is visible from all the directions up to a hemisphere, with n pointing to the 'north pole' and T being the 'equatorial' plane. As there are many points on the surface **S**, the intersection of all these hemispheres consists of all the directions from which the entire surface is visible. The resulting spherically convex region is called the visibility map (or Vmap) of the surface **S** [18].

Illustrative diagrams of the Vmap concept are shown in Fig. 2. It is intuitive that any point on the Vmap corresponds to a direction from which the entire surface is visible. As mentioned, a Vmap is a convex region on a unit sphere as shown in Fig. 2(b) and (c). In Fig. 2(b), the Vmap of a plane is a hemisphere as shown in Fig. 2(b) as shaded. That is, standing at any point on the shaded

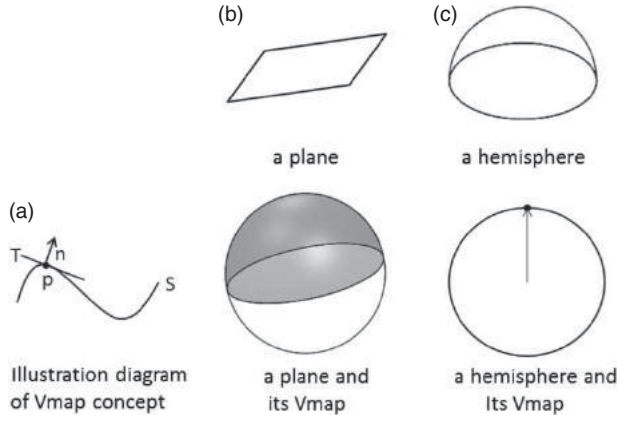

Figure 2. Illustration diagrams of Vmap concept with examples.

hemisphere, the entire plane is visible. In Fig. 2(c), it shows the Vmap of a hemispherical surface. The Vmap is only a single point at the "north pole" of the unit sphere. That is, only when standing on the north pole, the entire hemispherical surface is visible.

2.3. Visibility capacity

Visual capacity is a term used to describe a manufacturing process. It is determined by its visual style and visual field. Different manufacturing processes have different visual styles, and different visual styles could do different unit work in manufacturing. The visual style of a manufacturing effector is categorized by their topological dimensionalities as shown in Fig. 3. The first style is 0 Dimension, called point visual style as shown in Fig. 3(a). Most machining processes have point visual style. The second is 1D line/curve visual style shown in Fig. 3(b). A typical example of such manufacturing process is electric discharge wire-cutting. The third is 2D plane/surface visual style shown in Fig. 3(c). This style refers to manufacturing processes such as die casting, molding, forging, and so on.

The visual field of manufacturing effectors is related to the degree of freedom (DOF) of a manufacturing process. Normally, the DOF of manufacturing processes could be categorized to the range from 1 DOF to 5 DOFs. Casting, molding and forging et al have 1DOF; electric discharging machining has 2 DOF; and numerical controlled machining (CNC) could have 3 DOF, 4 DOF, or 5 DOF. The number of DOF of a manufacturing process decides the viewing directions of manufacturing effectors. When the visual style and visual field of a manufacturing effector are given, the visual capacity of a manufacturing process is defined.

The visual capacity of manufacturing processes could also be expressed on the unit sphere. An illustrative diagram about visual capacity (defined by visual style and

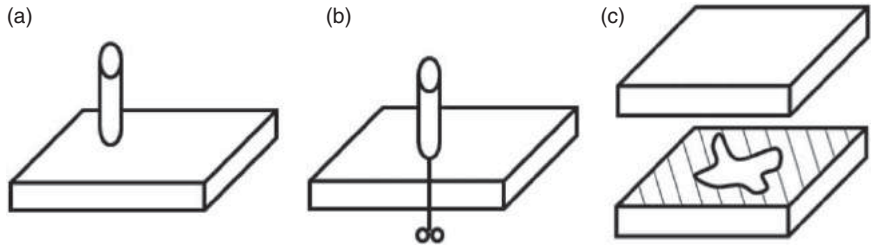

Figure 3. Visual style by topological dimensionality.

Table 1. Unit sphere expressions of visual capacity.

Visual Styles	*Visual Fields*		
Surface	1DOF	2DOF	3DOF
Line	2DOF	3DOF	4DOF
Point	3DOF	4DOF	5DOF
Unit sphere expressions of visual capacity	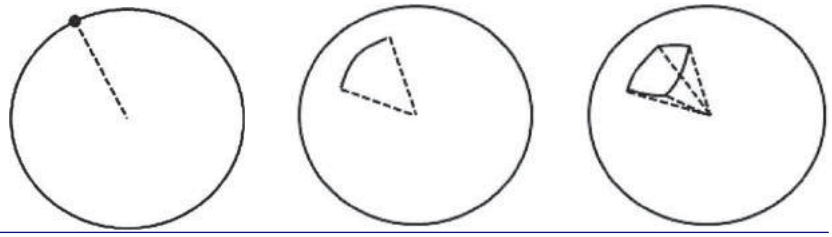		

visual field) on a unit sphere is shown in Tab. 1. Take a manufacturing process with "1 DOF" visual field and "Surface"visual style as an example, its visual capacity is just a point on the unit sphere. That is, the manufacturing process has just one manufacturing direction. The practical examples of this kind of process include casting, molding and so on. Now, take a 3-axis CNC machining process as an example. It has a "Point" visual style and "3 DOF" visual field. Its visual capacity is also a point on the unit sphere. That is, the tool can only access the object from one direction. For the case of 5-axis CNC machining, it has a "Point" visual style and a "5 DOF" visual field. Its visual capacity is represented as a spherical polygon region on the unit sphere.

Since the Vmap (Fig. 4(a)) of an object and the visual capacity (Fig. 4(b)) of a manufacturing process are both expressed on a unit sphere, they can be overlapped as concentric spheres as shown in Fig. 4(c). Now, if the visual capacity (represented as the thick lines) intersects with all Vmap (represented as thinner lines) in Fig. 4(c), then the part is manufacturable. Otherwise, the non-intersected Vmap will not be manufacturable.

3. Topology optimization with visibility constraints

Today there are a number of topology optimization schemes in use. They include Genetic Algorithms (GA) based [4,6,7], Solid Isotropic Material with Penalization (SIMP) based [1,14], level set based[13,17,19], and Particle Swarm Optimization (PSO) based [11,15] etc. Of all the schemes, SIMP based methods have been favored in most applications due to their fast convergence rate and stable solutions. Therefore, in this study, the proposed topology optimization approach is developed based on the SIMP scheme.

3.1. The SIMP algorithm

Generally, a topology optimization problem for minimum compliance could be expressed as Eqn(1):

$$\begin{aligned} &\min_{\mathbf{u},\rho_e} : c_{(\rho)} = \mathbf{f}^T\mathbf{u} \\ &s.t. \ : \left(\sum_{e=1}^{N} \rho_e^p \mathbf{K}\right)\mathbf{u} = \mathbf{f}, \\ &\quad : \sum_{e=1}^{N} v_e\rho_e \le V, \\ &\quad : 0 < \rho_{\min} \le \rho_e \le 1, \quad e = 1,\ldots,N. \end{aligned} \tag{1}$$

Where $c_{(\rho)}$ is the compliance of the structure. $\mathbf{f}$, $\mathbf{u}$ and $\mathbf{K}$ are the global load, global displacement and stiffness matrix respectively. ρ_e indicates the relative density of each element; $\rho_{\min}$ represents the minimum relative density. p is the penalization index which is normally assigned to 3. N is the number of elements. v_e is the element's volume and V is the total volume of the design domain.

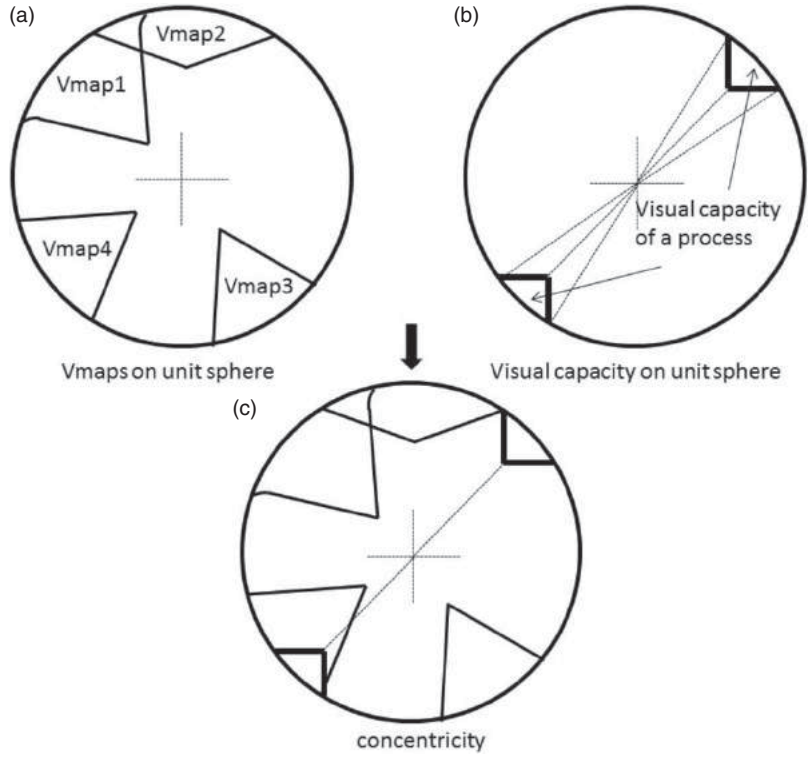

Figure 4. Concentric spheres of Vmaps and visual capacity.

The SIMP scheme uses an Optimality Criteria method to update relative densities. The formulation of this process is expressed in Eqn (2):

$$\rho_{K+1} = \begin{cases} \max\{(1-\zeta)\rho_K, \rho_{\min}\} \\ \quad if \quad \rho_K B_K^{\eta} \le \max\{(1-\zeta)\rho_K, \rho_{\min}\}, \\ \min\{(1+\zeta)\rho_K, 1\} \\ \quad if \quad \min\{(1+\zeta)\rho_K, 1\} \le \rho_K B_K^{\eta}, \\ \rho_K B_K^{\eta} \\ \quad otherwise. \end{cases} \tag{2}$$

Where η is the damping coefficient with a value assigned to 0.5; ζ is the move limit with value assigned to 0.2. These values are determined based on experiments of Sigmund and Bendsoe. In Eqn(2), the variable B_K could be obtained by Eqn(3) as follow:

$$B_K = \frac{-\dfrac{\partial c}{\partial \rho_e}}{\lambda \dfrac{\partial V}{\partial \rho_e}} \tag{3}$$

In Eqn(3), λ is a Lagrangian multiplier which is decided by a bi-sectioning method. The sensitivity of the objective function $\partial c/\partial\ \rho_e$ could be computed by Eqn(4) as:

$$\frac{\partial c}{\partial \rho_e} = -p(\rho_e)^{p-1} \mathbf{u}_e^T \mathbf{k}_e \mathbf{u}_e \tag{4}$$

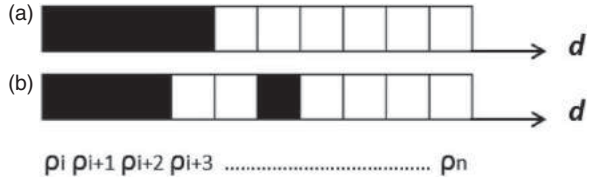

Figure 5. An element's visibility in a given direction d.

3.2. Visibility constraints in topology optimization

When the design space is converted to a finite element environment, the visibility could be described by using Fig. 5. In a given direction **d**, the boundary element is visible if the solid elements are lined as shown in Fig. 5(a). On the contrary, Fig. 5(b) shows a structure with invisible boundary elements (the white elements in between black elements) in direction **d**.

Therefore, given a manufacturing direction **d**, if the boundary element in this direction is visible, the following equation about element densities must be satisfied:

$$\rho_i \ge \rho_{i+1} \ge \cdots \ge \rho_n \tag{5}$$

Using Eqn(5) as constraint in the above described topology optimization algorithm, the resulting structure will be visible from the given direction.

4. Mapping visual capacity onto a discrete unit sphere

Now, the problem is how to define the manufacturing directions. Refer to Tab. 1, the visual capacity of a manufacturing process is defined on a unit sphere. In this paper, the unit sphere is discretized by dividing it along longitude and latitude as shown in Fig. 6. Each intersection point between a longitude and a latitude line represents a potential manufacturing direction. Of course, the more longitude and latitude lines we use, the higher accuracy the sphere discretization will be. There is always a compromise between accuracy and computational complexity.

Suppose we have m longitude lines and n latitude lines, the total number of intersection point can be represented as a two dimensional array S[i,j] where i = [1,m] and j = [1,n]. Since the south pole and north pole each converges to a single point, they are represented independently as Ps and Pn. Now, the visual capacity of a manufacturing process can be mapped to finite points on the unit sphere.

Now the pseudo code for running the topology optimization is shown in the following:

Initialize S[j,j]
Construct visual capacity V_{CAP}
For i = 1 to m,
For j = 1,n
Check intersection between S[i,j] and V_{CAP},
If yes, S[i,j] = 1 / map the* V_{CAP} *to a 2D array */*
Otherwise S[i,j] = 0
Endloop j
Endloop i
For i = 1 to m, and j = 1 to n
If S[i,j] = 1
Run SIMP based constrained optimization
End

5. Sample studies

The following will show two examples of topology optimization with different visibility constraints. All of these visibility constraints can be mapped to practical manufacturing processes. The computer system used for these computations is based on an Intel(R) Core(TM)2 with Duo CPU E8500 @ 3.16 GHz, and 8GB RAM memory. The programming environment is MATLAB 7.10.0 (R2010a).

5.1. Unidirectional constraint

Firstly, take 3-axis CNC machining as an example, this process has a point visual capacity. Without re-setups, this process has just one direction (a point on the unit sphere) which is vertical downward as shown in Fig. 7(a).

The load & boundary conditions of an example is shown in Fig. 7(b). This design domain is divided into a 10*20*20 mesh. The four bottom corners are fixed as

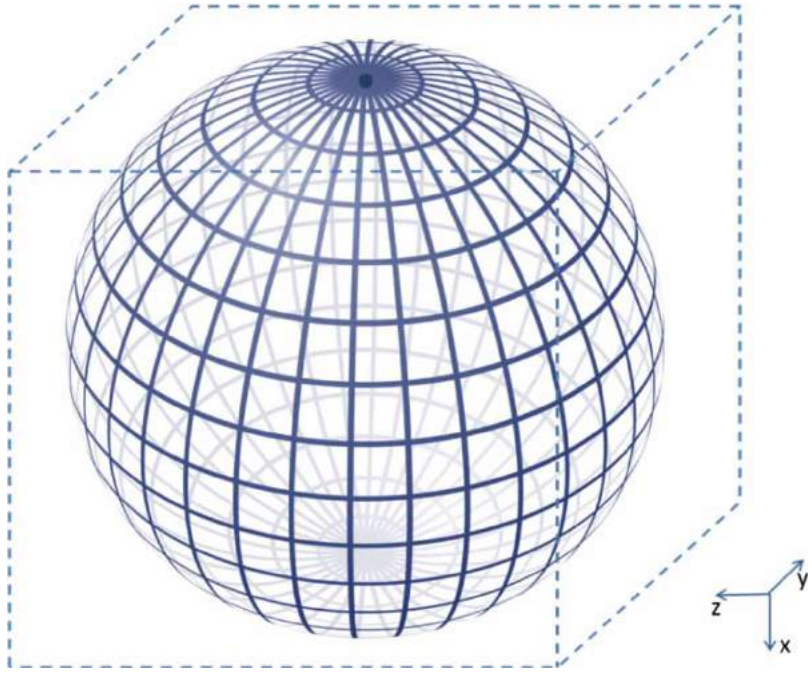

Figure 6. Discretizing a unit sphere.

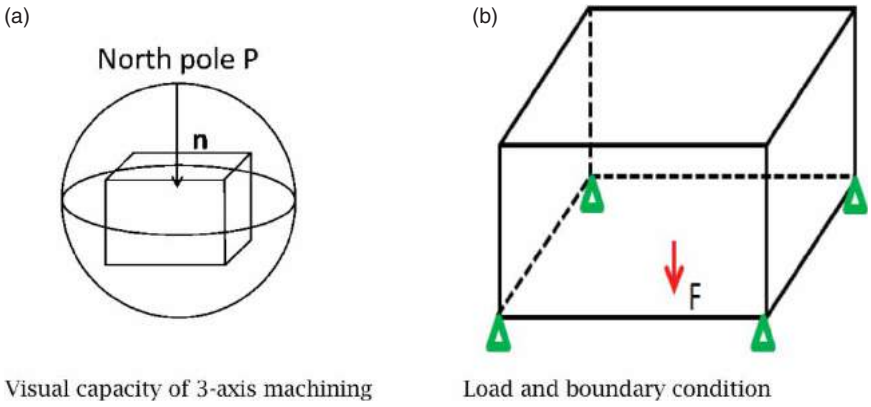

Figure 7. Unidirectional load and visual capacity.

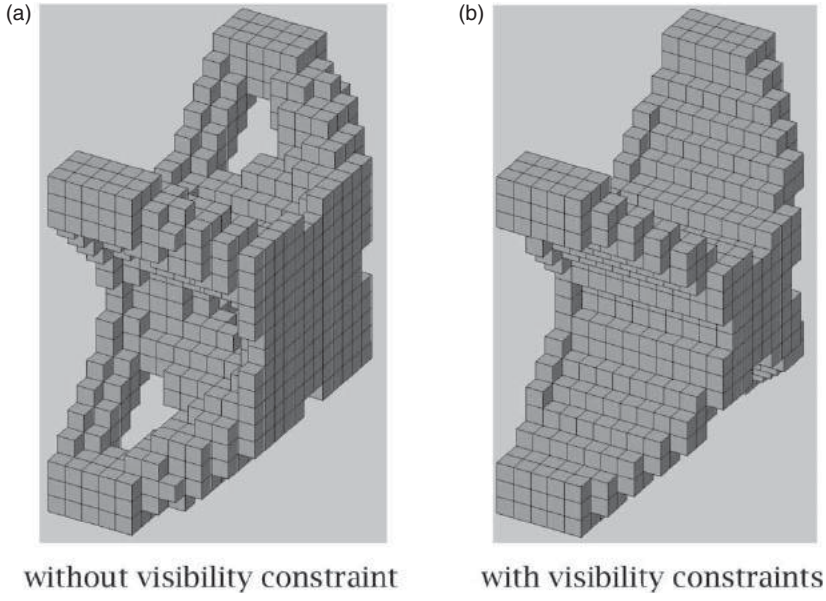

Figure 8. Topology optimization results for sample 1.

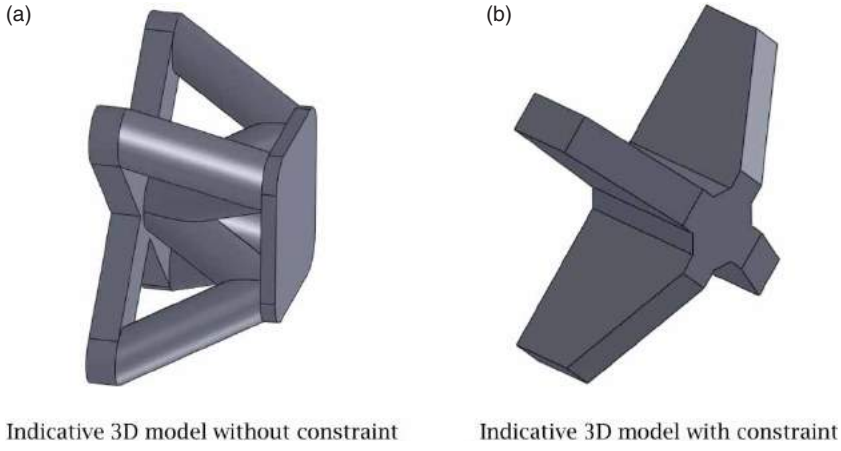

Figure 9. Optimization results converted into 3D models.

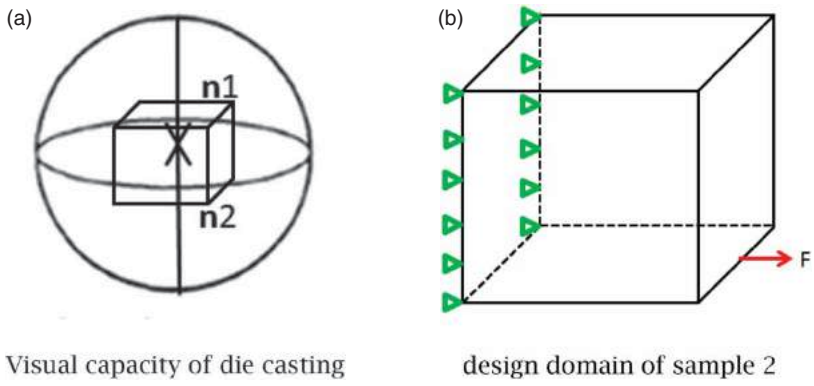

Figure 10. Topology optimization with bidirectional constraints.

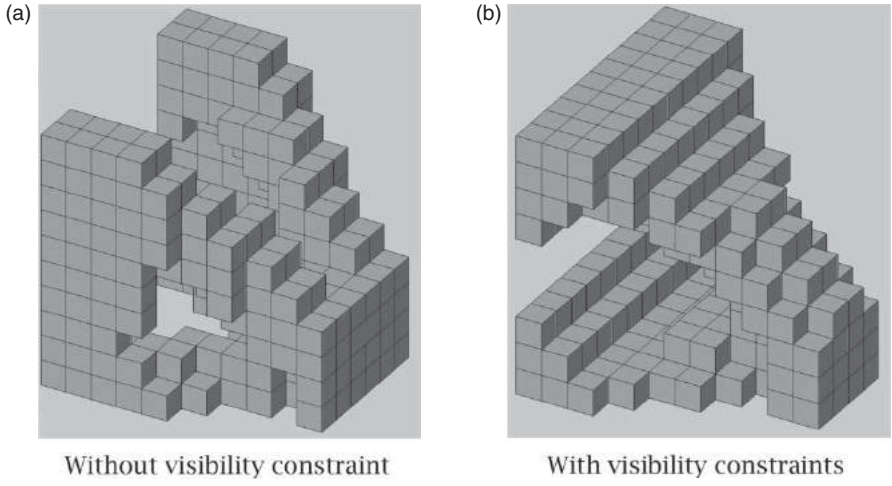

Figure 11. Topology optimization results for sample 2.

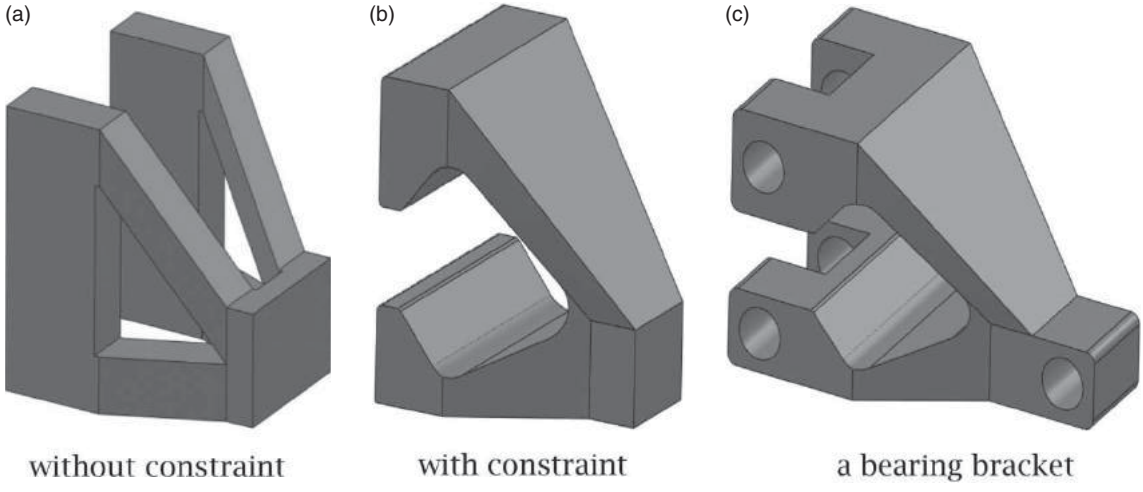

Figure 12. Optimization results converted into 3D models.

shown by the green triangle, and a load F is added at the center of bottom surface.

The optimization results without and with unidirectional constraint are shown in Fig. 8. The number of iteration for the topology optimization without and with constraint is 13 and 14 respectively. The compliance of the results is 4.576 and 5.4537 for optimization without constraints and with constraint respectively. The iteration takes approximately 982 seconds for without constraints and 1206 seconds when constraints are added. As shown in Fig. 8(a), the result without constraint is complicated and cannot be manufactured using 3-axis machining. In comparison, the result with unidirectional constraint as shown in Fig. 8(b) is much simpler and easily manufacutrable by 3-axis CNC machining. In order to show the results in a better form, the discrete results are converted into illustrative 3D models as shown in Fig. 9. Again, it can be seen that the result with visibility constraints (Fig. 9(b)) is much better in terms of design and manufacturing. Currently, the conversion of the discrete model into a 3D model is done manually. The authors are also developing methods for automatic 3D model re-construction from the discrete result.

5.2. Bidirectional constraints

Another example is for die casting, which has a 1DOF surface visual capacity. Because die casting has a parting surface with two draw directions, therefore its visibility direction set has two inverse directions n1 and n2 as shown in Fig. 10(a). The bidirectional constraint is added to the design domain as shown in Fig. 10(b).

In this sample study, the design domain is divided into a 10*10*10 mesh. The green triangles in Fig. 10(b) are the fixed edges. The red arrow represents the load.

After optimization, the results without and with bidirectional constraint are shown in Fig. 11. The number of iteration in running the topology optimization is 10 and 14 for without constraints and with constraints respectively. Without constraint, the resulting structure in Fig. 11(a) needs at least three manufacturing directions, which means that side cores are needed. Using the bidirectional constraint, the resulting structure is shown in Fig. 11(b). It could be manufactured by a normal mold without the need of side cores. Again, the indicative 3D models of the optimized results are shown in Fig. 12. Obviously, the result without constraint in Fig. 12(a) is more complicated and more difficult to manufacture. The constrained result shown in Fig. 12(b) is simpler and similar to a commonly used mechanical part such as a bearing bracket shown in Fig. 12(c).

6. Conclusions & future works

This study attempts to develop a general approach for topology optimization in mechanical design so that part generated could be manufactured by the intended manufacturing processes. Visibility is thought to be well associated with manufacturing capabilities of most manufacturing processes. It is thus used to constrain the topology optimization such that the resulting part could be manufactured cost effectively. Two samples have been used to show the effectiveness of the proposed approach in generating results with simple geometry and good manufacturability.

In this paper, only point visual capacity manufacturing processes are presented. In future works, the line and surface visual style for manufacturing processes such as 5-axis CNC machining will be further studied. Meanwhile, in order to fully consider manufacturability, accessibility (with consideration of tool geometry and size) must be taken into consideration together with visibility because even if a surface is visible by the effector, the interferences between the effector and the workpiece surface could still make the surface inaccessible, thus not manufacturable.

Acknowledgement

The research reported in this paper is supported by an HKU small project grant.

ORCID

Yonghua Chen http://orcid.org/0000-0003-4020-1977

References

[1] Bendsoe, M.P.; Sigmund, O.: Topology Optimization: Theory, Methods and Applications. Springer-Verlag, 2003.

[2] Chang, K.H.; Tang, P.S.: Integration of design and manufacturing for structural shape optimization, Advances in Engineering Software, 32, 2001, 555–567. http://dx.doi.org/10.1016/S0965-9978(00)00103-4.

[3] Chen, L.L; Chou, S.Y.; Woo, T.C.: Parting directions for mould and die design, Computer-Aided Design, 25(12), 1993, 762–768. http://dx.doi.org/10.1016/0010-4485(93)90103-U.

[4] Hajela, P.; Lee, E.: Genetic algorithms in truss topology optimization, International journal of solids and structures, 32, 1995, 3341–3357. http://dx.doi.org/10.1016/0020-7683(94)00306-H.

[5] Harzheim, L.; Graf. G.: A review of optimization of cast parts using topology optimization, Struct. Multidisc. Optim., 30, 2005, 491–497. http://dx.doi.org/10.1007/s00158-005-0553-x.

[6] Huang, X.; Xie, Y.M.: Evolutionary topology optimization of continuum structures, New York, John Wiley and Sons, 2010. http://dx.doi.org/10.1002/9780470689486.

[7] Kennedy, J.; Eberhart, R.: Particle swarm optimization, Proceedings of the IEEE International Conference on Neural Networks, Perth Australia, November 27–30, 1995, Vol.4, 1942–1948. http://dx.doi.org/10.1109/ICNN.1995.488968.

[8] Krog, L.; Tucker, A.; Rollema, G.: Application of topology, sizing and shape optimizationmethods to optimal design of aircraft components, Altair Engineering, 2011, http://www.altairpd.com.

[9] Lu, J.; Chen, Y.: Topology optimization and customization of a prosthetic knee joint design, International Journal of Computer Integrated Manufacturing, 26(10), 2013, 968–976. http://dx.doi.org/10.1080/0951192X.2011.652178.

[10] Niclas, S.: Topology optimization of structures with manufacturing and unilateral contact constraints by minimizing an adjustable compliance–volume product, Struct. Multidisc. Optim., 42, 2010, 341–350. http://dx.doi.org/10.1007/s00158-010-0502-1.

[11] Padhye, N.: Topology optimization of compliant mechanism using multi-objective particle swarm optimization, Proceedings of the 2008 GECCO conference companion on Genetic and evolutionary computation. Atlanta, USA, July 12–16, 2008, 1831–1834. http://dx.doi.org/10.1145/1388969.1388983.

[12] Schmidt, T.; Lauber, B.: Topology optimization and casting: a perfect combination, ANSYS Advantage, Vol. 3(1), 2009, 42–43.

[13] Sethian, J.A.: Level set methods and fast marching methods: evolving interfaces in computational geometry, fluid mechanics, computer vision, and materials science, 1999, Cambridge University Press.

[14] Sigmund, O.: A 99 line topology optimization code written in MATLAB, Structural and Multidisciplinary Optimization, 21, 2001, 120–127. http://dx.doi.org/10.1007/s001580050176.

[15] Tseng, K.Y.; Zhang, C.B.; Wu, C.Y.: An enhanced binary particle swarm optimization for structural topology optimization, IMechE Proc Part C Journal of Mechanical Engineering Science, 227(7), 2010, 2271–2287. http://dx.doi.org/10.1243/09544062JMES2128.

[16] Wang, L.; Basu, P.K.; Leiva, J.P.: Automobile body reinforcement by finite element optimization, Finite Elements in Analysis and Design, 40(8), 2004, 879–893. http://dx.doi.org/10.1016/S0168-874X(03)00118-5.

[17] Wang, M.Y.; Wang, X.: "Color" level sets: a multi-phase method for structural topology optimization with multiple materials, Comput. Methods Appl. Mech. Engrg., 193, 2004, 469–496. http://dx.doi.org/10.1016/j.cma.2003.10.008.

[18] Woo, T.C.: Visibility maps and spherical algorithms, Computer-Aided Design, 26(1), 1994, 6–15. http://dx.doi.org/10.1016/0010-4485(94)90003-5.

[19] Yamada, T.; Izui, K.; Nishiwaki, S.; Takezawa, A.: A topology optimization method based on the level set method incorporating, Comput. Methods Appl. Mech. Engrg., 199, 2010, 2876–2891. http://dx.doi.org/10.1016/j.cma.2010.05.013.

[20] Zhou, M.; Shyy, Y.K.; Thomas, H.L.: Topology optimization with manufacturing constraints, Proceedings of the 4th World Congress of Structural and Multidisciplinary Optimization, Dalian, China, June 4–8, 2001.

[21] Zuo, K.T.; Chen, L.P.; Zhang, Y.Q.; Yang, J.: Manufacturing and Machining–based topology optimization, International Journal of Advanced Manufacturing Technology, 27, 2006, 531–536. http://dx.doi.org/10.1007/s00170-004-2210-8.